# Targeted Vault Nanoparticles Engineered with an Endosomolytic Peptide Deliver Biomolecules to the Cytoplasm

**Muri Han,[†] Valerie A. Kickhoefer,[†] Glen R. Nemerow,[‡] and Leonard H. Rome[†,§,*]**

[†]Department of Biological Chemistry, David Geffen School of Medicine at UCLA, Los Angeles, California 90095, United States, [‡]Department of Immunology and Microbial Science, The Scripps Research Institute, La Jolla, California 92037, United States, and [§]California NanoSystems Institute at UCLA, Los Angeles, California 90095, United States

**ABSTRACT** Vault nanoparticles were engineered to enhance their escape from the endosomal compartment by fusing a membrane lytic peptide derived from adenovirus protein VI (pVI) to the N-terminus of the major vault protein to form pVI-vaults. We demonstrate that these pVI-vaults disrupt the endosomal membrane using three different experimental protocols including (1) enhancement of DNA transfection, (2) co-delivery of a cytosolic ribotoxin, and (3) direct visualization by fluorescence. Furthermore, direct targeting of vaults to specific cell surface epidermal growth factor receptors led to enhanced cellular uptake and efficient delivery of vaults to the cytoplasm. This process was monitored with fluorescent vaults, and morphological changes in the endosomal compartment were observed. By combining targeting and endosomal escape into a single recombinant vault, high levels of transfection efficiency were achieved using low numbers of vault particles. These results demonstrate that engineered vaults are effective, efficient, and nontoxic nanoparticles for targeted delivery of biomaterials to the cell cytoplasm.

**KEYWORDS:** vaults · nanoparticles · delivery · targeting · adenovirus · protein VI · cytosolic release

A number of different platforms have been developed as therapeutic delivery systems including viruses,[1] liposomes,[2−4] polymers,[5−7] proteins,[8,9] and various inorganic materials.[10,11] Although some of these systems have shown promise *in vitro*, their *in vivo* utilization has been hampered by unwanted properties (*e.g.*, immunotoxicity, poor release of drug, mistargeting, instability, *etc.*).[12−16] Consequently, when one evaluates a new therapeutic delivery system, it is necessary to evaluate a number of criteria including safety, capacity, targeting, and pharmacokinetics.

Vaults are naturally occurring cytoplasmic ribonucleoprotein particles that are structurally conserved among most eukaryotes.[17] Mammalian vaults are composed of multiple copies of the 97-kDa major vault protein (MVP)[18] which constitutes ~75% of the total protein mass, the 193-kDa vault poly(ADP-ribose) polymerase (VPARP),[19] the 290-kDa telomerase-associated protein-1 (TEP1),[20] and one or more small untranslated RNAs (vRNA).[21−23] Vault function remains unknown. The basic vault structure can be recapitulated by expression of MVP alone in insect cells where particles self-assemble from multiple MVP subunits.[24] The recombinant vault nanoparticle has properties which are desirable for drug/gene delivery including (1) a hollow, barrel-like structure with overall dimensions of 72.5 × 41 × 41 nm$^3$, and a large internal cavity (5 × 10$^4$ nm$^3$)[25,26] which can encapsulate biomaterials for their transportation,[27−29] (2) nonimmunogenic/nontoxic composition,[30] (3) ease of modification of either termini of MVP[25,31] (see following), and (4) a dynamic structure[32−35] able to "breathe" in solution, making it very useful for the release of biomaterials.

Schematic diagrams of the vault structure and vaults engineered with additional amino acids fused at the N- and C-termini of MVP are shown in Figure 1A. Vaults assemble into halves from 39 or more copies of MVP with the MVP N-terminus at the waist and the MVP C-terminus at the cap.[25,26,36] Two half vaults assemble into the complete vault particle. When N-terminal peptide extensions are added to MVP (shown in red), recombinant vaults are formed with these peptides facing the interior of the particles at the waist[25] (shown as light red in the assembled particle to indicate that these added peptides are inside the particle). When C-terminal peptide extensions are added to MVP (shown in blue), recombinant vaults are formed with these peptides accessible on the exterior surface of the

* Address correspondence to lrome@mednet.ucla.edu.

Received for review December 3, 2010 and accepted July 8, 2011.

**Published online July 09, 2011**
**10.1021/nn2014613**

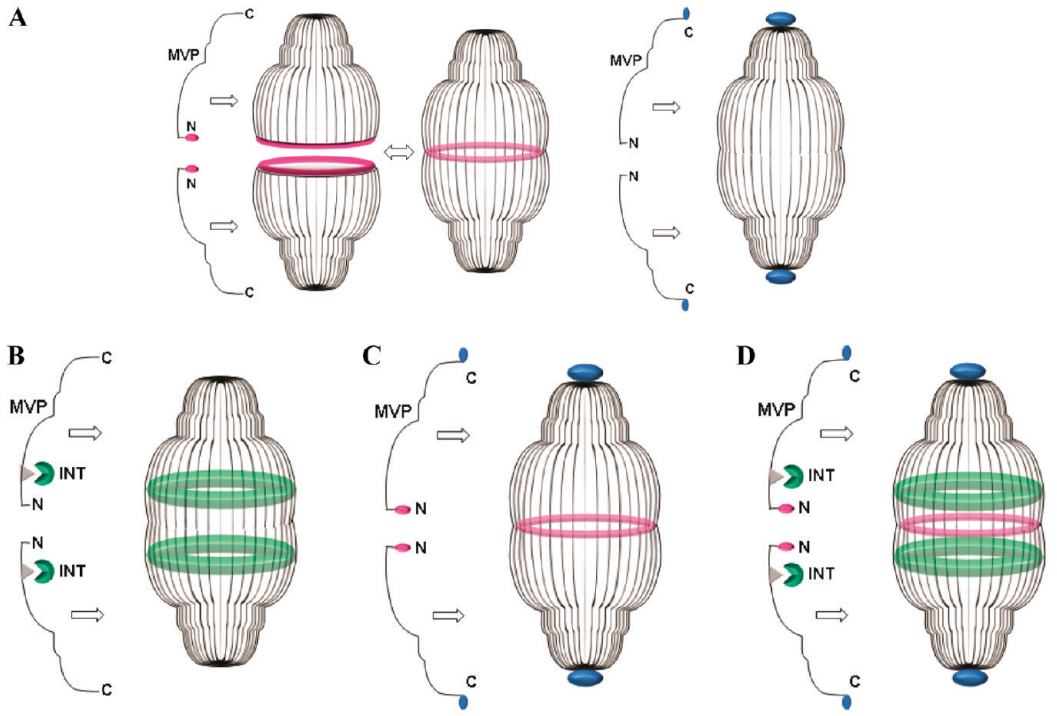


**Figure 1. Schematic diagrams of engineered vault structures. (A) Vaults engineered with additional amino acids at the N- and C-termini of the major vault protein (MVP). N-terminal peptide extensions (shown in red) fused to MVP are located on the interior surface of the engineered vault particles at the waist (shown as light red in the assembled particle to indicate that these peptides are located inside the particle). C-terminal peptide extensions (shown in blue) fused to MVP are located on the exterior surface of the particles at the end of the caps. (B) Vaults engineered with exogenous protein fused to the INT. The INT binding site on MVP (shown as a gray triangle) is located above and below the waist of the vault facing the inside of the particle. Packaged proteins fused to the INT domain are displayed as two rings (shown in green) bound to the INT binding sites on the interior of vaults. (C) Diagram of multifunctional vaults that contain both N- and C- terminal peptide extensions as indicated. (D) Diagram of multifunctional vaults containing INT fusion proteins.**

particles at the caps.[31] In a previous study, these peptides were used to target vaults to the cell surface epidermal growth factor (EGF) receptors, either directly or when complexed with an antibody that binds to the external portion of the EGF receptor (EGFR).[31,37] Exogenous proteins can be packaged into vault particles when fused to the MVP interaction domain (INT) derived from VPARP (amino acids 1563−1724) (Figure 1B, shown in green).[27] The INT binding site has been mapped to a region on each MVP that is located above and below the waist of the vault facing the inside of the particle (Figure 1B).[27,38,39] The location of this site is marked as a gray triangle on the MVP. Previous studies demonstrated that vaults are dynamic particles able to breathe in solution, exchange halves, and interact with the cellular milieu, thus allowing materials and peptides bound to the interior of the particle to interact with the cellular environment.[33,35] We recently demonstrated that a vault packaged with a chemoattractant, CCL21, led to tumor infiltration by lymphocytes and decreased tumor growth in an animal model for lung cancer.[40] In addition, vault particles engineered to package the drug, all-*trans* retinoic acid, retain the ability to kill HepG2 cancer cells *in vitro*.[41]

For the vault to be an effective and versatile delivery vehicle, it should be able to release packaged therapeutic materials into the cytosol of targeted cells to prevent undesirable side effects and/or degradation in lysosomes. Following adenovirus internalization, the endosomal membrane is disrupted by an endosomolytic adenoviral protein (pVI).[42] To enhance cytosolic release of biomaterials from vaults, the membrane lytic domain of adenovirus pVI was fused to the INT packaging domain and assembled into recombinant vaults (pVI-INT/MVP vaults).[43] Vault particles packaged with pVI-INT were required at a high concentration (>$10^6$ particles per cell) for nonspecific delivery of biomaterials to mouse macrophage RAW 264.7 cells through phagocytosis. In the present study we show that when vaults packaged with pVI-INT are specifically targeted to the EGF receptor, biomaterials are delivered to cells at higher transfection efficiency than with either calcium phosphate alone or a commercial transfection reagent. Furthermore, by combining the targeting domain and a 20 amino acid membrane lytic domain of pVI into a single vault structure, a highly efficient delivery vehicle is obtained that is not toxic. This vault nanoparticle retains its ability to package exogenous protein payloads, can target specific cell surface receptors, and is an effective tool for delivery of biomaterials to the cytosol.

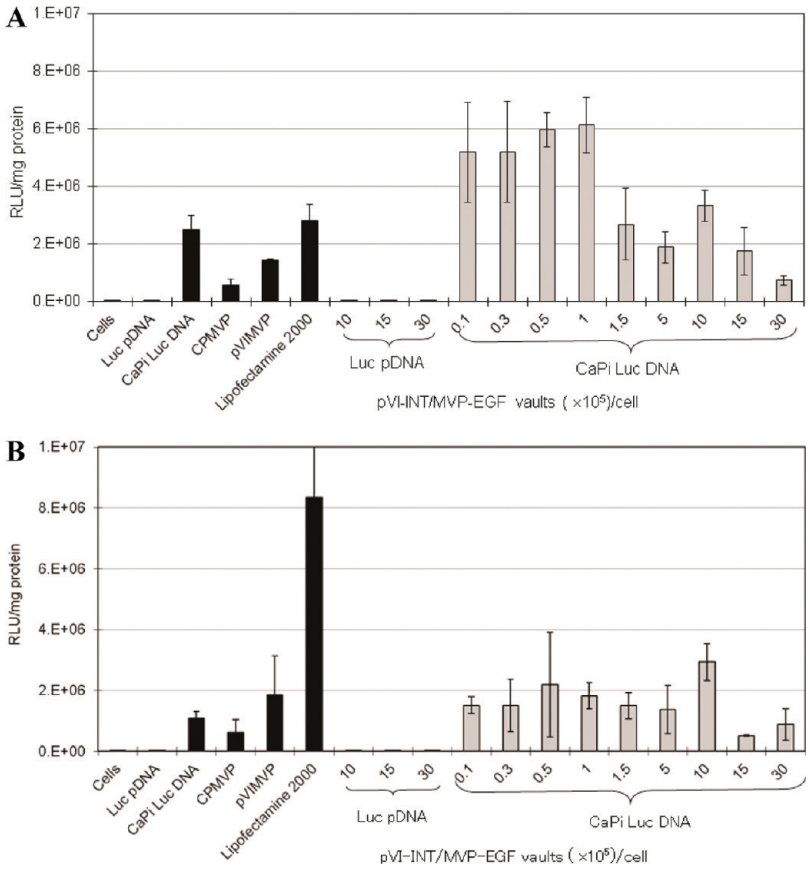


**Figure 2. Targeted co-delivery of calcium phosphate precipitated plasmid DNA encoding luciferase (CaPi Luc DNA) by EGF vaults containing pVI-INT (pVI-INT/MVP-EGF vaults). (A) Expression of co-delivered CaPi Luc DNA by the indicated numbers of pVI-INT/MVP-EGF vaults (gray bars) to A431 cells [that have >$10^6$ EGF receptors (EGFR) on their cell surface] was measured by luciferase assays. Controls (black bars) included cells only, Luc plasmid DNA (Luc pDNA) only, CaPi Luc DNA only, and CaPi Luc DNA with either CP-MVP vaults ($3 \times 10^6$ particles/cell) or pVI-MVP vaults ($3 \times 10^6$ particles/cell), Luc pDNA with Lipofectamine 2000, and Luc pDNA with indicated numbers of vaults. Luciferase assays were carried out 48 h "post-transfection" and were normalized to protein concentration. (B) The same analysis described in panel A was carried out using HeLa cells that have ~$10^4$ surface EGFR per cell.**

## RESULTS AND DISCUSSION

**Co-delivery of CaPi DNA by pVI-INT/MVP-EGF Vaults.** Although the mechanism remains unknown, calcium phosphate precipitated plasmid DNA (CaPi DNA) is an established, classical method for transfecting plasmid DNA (pDNA) into mammalian cells. In a previous study the coprecipitation of adenoviral vector with CaPi DNA increased gene transfer into mouse dendritic cells, presumably by allowing cointernalized CaPi DNA access to the cytoplasm when endosomes were disrupted by the virus.[44] However, some cell types (for example stem cells) are resistant to transfection, due in part to inefficient endosomal escape and/or nuclear trafficking.[45,46] Adenoviral protein VI (pVI) mediates adenovirus escape from the endosome[42,47] as monitored by enhanced transfection by CaPi DNA.[43] We used this method to demonstrate endosomal escape mediated by pVI-containing vaults.

Vault particles packaged with pVI-INT facilitated delivery of CaPi DNA to mouse macrophage RAW 264.7 cells presumably through nonspecific phagocytic uptake.[43] Receptor targeted vaults engineered to display EGF (MVP-EGF vaults) on their external surface can specifically bind to EGFR on epidermal carcinoma A431 cells.[31] To determine whether targeting vaults would enhance transfection of CaPi DNA encoding luciferase (CaPi Luc DNA), the pVI-INT fusion protein was packaged into the lumen of MVP-EGF vaults (pVI-INT/MVP-EGF). We compared the ability of these vaults to facilitate plasmid transfection of HeLa (~$10^4$ surface EGFR per cell) and A431 (>$10^6$ EGFR per cell) cells, as these vaults bind EGFR (Figure 2). An increase in transfection efficiency was observed that exceeded that of a commercial transfection reagent, Lipofectamine 2000, and CaPi Luc DNA. The highest level of targeted transfection efficiency was seen with $0.1 \times 10^5$ to $1 \times 10^5$ vaults/cell in A431 cells (Figure 2A). Higher numbers of pVI-INT/MVP-EGF vaults induced lower transfection efficiencies probably due to the general toxicity of the pVI. When HeLa cells were examined, the transfection efficiency of this vault structure was lower than Lipofectamine 2000 (Figure 2B). As HeLa cells display fewer copies of EGFR than A431 cells, this result suggests that

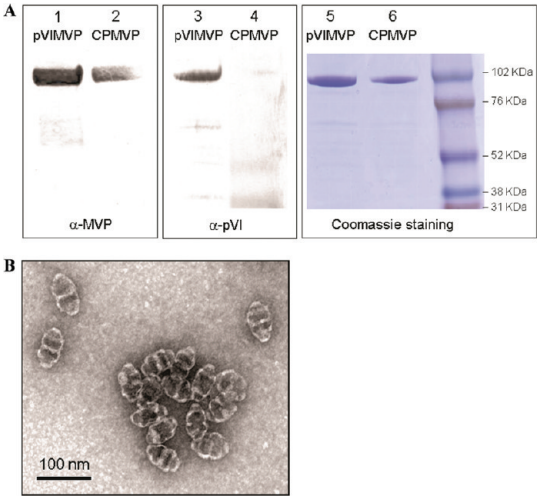


**Figure 3. Analysis of pVI-MVP recombinant vaults. (A) Purified pVI-MVP vaults (lanes 1, 3, and 5) and CP-MVP vaults (lanes 2, 4, and 6) were fractionated by SDS-PAGE and analyzed by Western blot (lanes 1−4) or stained with Coomassie (lanes 5 and 6). The blot from lanes 1 and 2 was probed with an anti-MVP polyclonal antibody, and the blot from lanes 3 and 4 was probed with an anti-pVI polyclonal antibody to confirm the presence of the pVI tag. (B) A representative electron micrograph of negative-stained recombinant pVI-MVP vault particles. Vaults were absorbed on carbon-coated copper grids for 5 min and stained with 1% uranyl acetate in water for 5 min. Dried samples were visualized using a JEM 1200-EX transmission electron microscope (JEOL, Tokyo, Japan).**

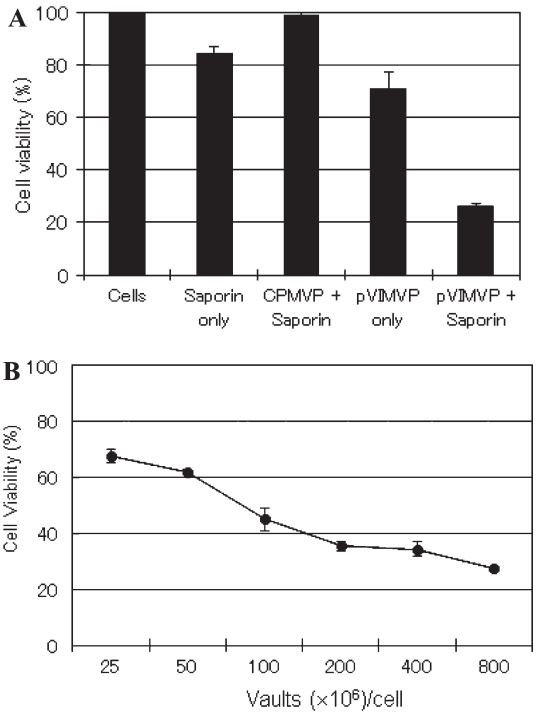


**Figure 4. Co-delivery of a ribotoxin (saporin) using pVI-MVP vault particles. (A) RAW 264.7 cells were incubated either alone, or with saporin ($1.65 \times 10^{-7}$ M) only, or with pVI-MVP vaults ($8 \times 10^8$ particles/cell) alone or with saporin, or with CP-MVP ($8 \times 10^8$ particles/cell) vaults and saporin, as indicated, and cell viability was measured 48 h later using the MTT assay. All values were normalized to untreated cells. (B) Dose response induced cytotoxicity in RAW 264.7 cells. Cells were incubated with the indicated numbers of pVI-MVP vaults in the presence of saporin ($1.65 \times 10^{-7}$ M) for 48 h prior to measuring viability by MTT.**

the high transfection efficiency of pVI-INT/MVP-EGF vaults in A431 cells resulted from facilitated co-delivery of CaPi Luc DNA to the cells mediated through the ligand−receptor protein interaction.

**An Alternative pVI Vault Design.** Although packaging pVI-INT inside of vaults has been shown to co-deliver various biomolecules,[43] it would be advantageous to develop a particle where the pVI domain is directly attached to the vault particle, leaving the lumen of the particle empty so that additional INT fusion proteins can be packaged inside of these vaults. Toward this goal, we fused a 20 aa lytic peptide derived from pVI (aa 34 to 53) directly onto the N-terminus of MVP (pVI-MVP vaults). In these vaults, the pVI is localized at the waist of the vault particle where other N-terminal tags have been previously shown to localize (Figure 1A).[25] Importantly, the INT binding site on MVP, located above and below the waist of the vault (Figure 1B), is available for binding of additional cargo into these vaults, thus adding another functional dimension.

Expression of pVI-MVP vaults in Sf9 insect cells was compared with that of vaults containing an N-terminal cysteine-rich (CP) peptide (CP-MVP vaults).[25] CP-MVP and pVI-MVP vaults were purified and analyzed by sodium dodecyl sulfate polyacrylamide gel electrophoresis (SDS-PAGE) (Figure 3A). Gels were either stained with Coomassie (Figure 3A, lanes 5 and 6) or immunoblotted with either an anti-MVP antibody (Figure 3A, lanes 1 and 2) or an anti-pVI antibody (Figure 3A, lanes 3 and 4). These results confirmed that pVI-MVP vaults were formed in Sf9 insect cells. Most vault purifications are carried out using 75 mM NaCl; however, the pVI-MVP vault structure was sensitive to salt concentration resulting in formation of some half-vault aggregates, previously described as vaultimers.[24] These aggregates could be mostly eliminated when vaults were purified using a salt concentration of 25 mM. These purified pVI-MVP vaults were examined by negative stain transmission electron microscopy (Figure 3B). The particles observed had the typical morphology of previously published intact monodispersed vault particles.[24]

**Co-delivery of Biomolecules by pVI-MVP Vaults into Macrophages.** We tested whether pVI-MVP vault particles were able to lyse the endosomal membrane by examining the co-delivery of a biomolecule into the cytosol of mouse macrophage RAW 264.7 cells, a cell line that readily phagocytoses particles (Figure 4). For this study, we used a soluble ribotoxin, saporin. Entry of saporin into the cytosol resulted in inhibition of protein synthesis and decreased cell viability. Saporin alone has low cell toxicity (<20%) due to its inability to cross the cell membrane (Figure 4A). Control vaults (CP-MVP) were

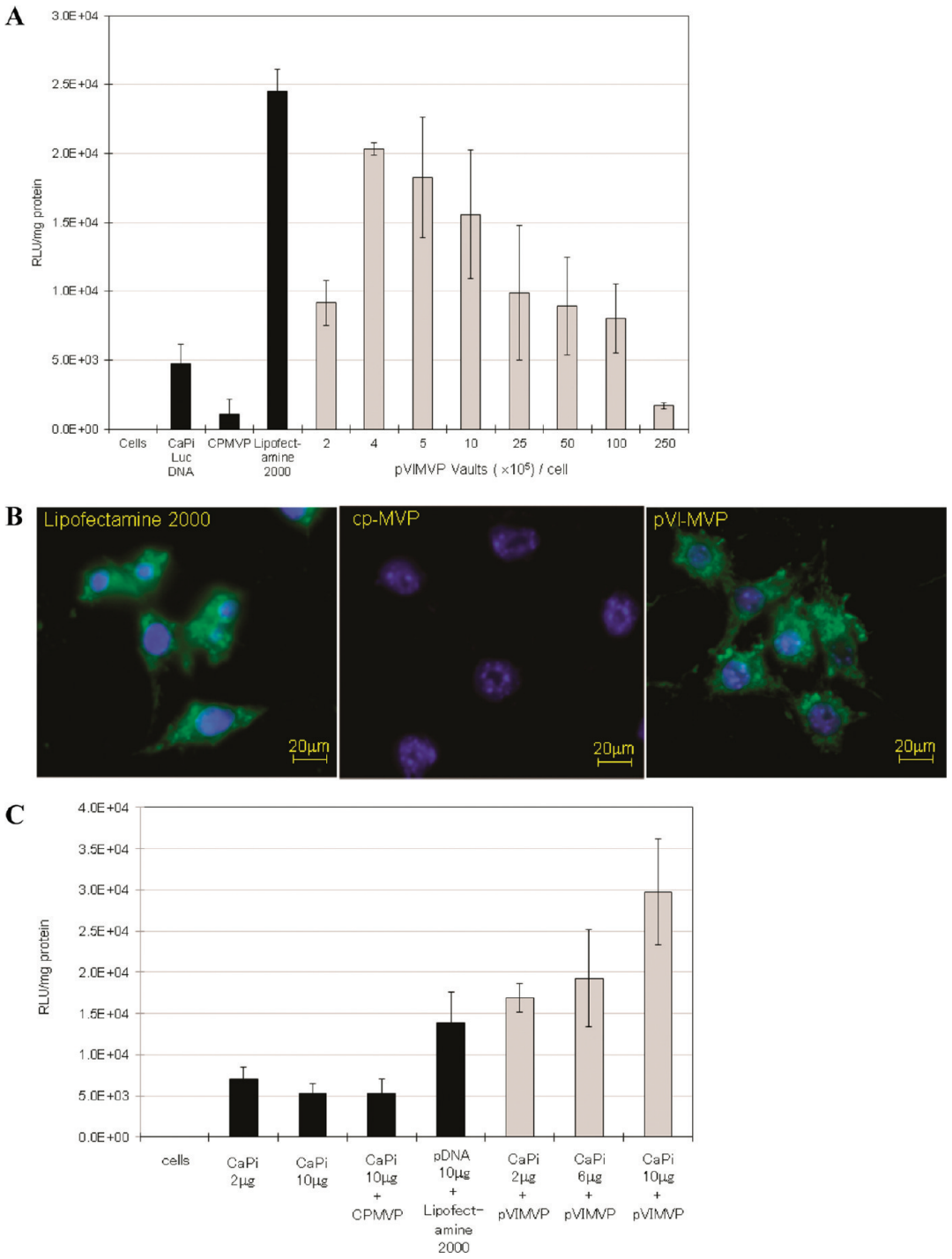


**Figure 5. Co-delivery of CaPi DNA by pVI-MVP vaults. (A) Transfection by the indicated amounts of pVI-MVP vaults (gray bars) with CaPi Luc DNA (2 $\mu$g/well) to RAW 264.7 cells. Controls (black bars) included CaPi Luc DNA alone, and CaPi Luc DNA with CP-MVP vaults ($2.5 \times 10^7$ particles/cell), and Luc pDNA with Lipofectamine 2000. (B) Comparison of expression of CaPi GL DNA (2 $\mu$g/well) cotransfected with either Lipofectamine (left panel), CP-MVP vaults ($4 \times 10^5$ particles/cell; center panel), or pVI-MVP particles ($4 \times 10^5$ particles/cell; right panel) into RAW 264.7 cells. (C) Cotransfection of the indicated amounts of CaPi Luc DNA with pVI-MVP vaults (gray bars, $4 \times 10^5$ particles/cell) into RAW 264.7 cells. Controls (black bars) included two different concentrations of CaPi Luc DNA alone, CaPi Luc DNA (10 $\mu$g/well) with CP-MVP vaults ($2.5 \times 10^7$ particles/cell), and Luc pDNA (10 $\mu$g/well) with Lipofectamine 2000.**

nontoxic, while pVI-MVP vaults alone at high concentrations ($8 \times 10^8$ particles per cell) decreased cell viability by ~30%, presumably due to a nonspecific interaction between the lytic pVI peptide and the plasma membrane. Co-delivery of the ribotoxin by pVI-MVP vaults decreased cell viability by greater than 70%. This effect was dose-dependent as indicated in Figure 4B. The ability of the pVI-MVP vaults to facilitate saporin toxicity is due to the concentration of the particles in endosomes where the natural breathing

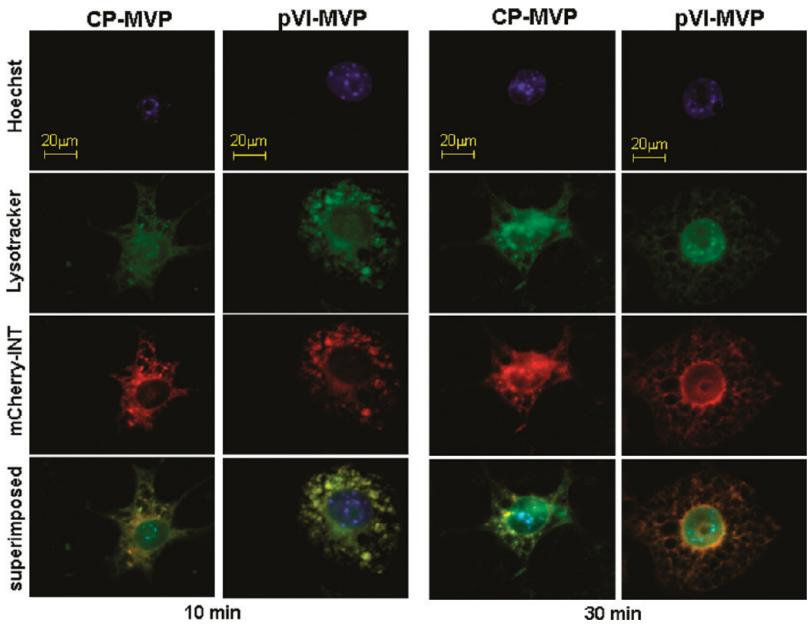


**Figure 6. Swelling and disruption of lysosomal membranes by pVI-MVP vaults in RAW 264.7 cells. Comparison of endocytosis of CP-MVP vaults containing mCherry-INT and pVI-MVP vaults containing mCherry-INT following incubation for 10 and 30 min. The nuclei were stained with Hoechst (blue). The lysosomes were stained with Lysotracker (green). The observed red fluorescence is the intrinsic fluorescence from the mCherry-INT protein packaged inside of the vaults. The low level of green fluorescence seen in the nucleus of the cells in 30 min is likely from autofluorescence which appears enhanced by the longer exposure times due to low cytoplasmic Lysotracker staining.**

of the vaults allows the pVI peptide to be exposed to the endosomal membrane resulting in lysis and release of vault particles and the ribotoxin into the cytosol.

We also evaluated the co-delivery of CaPi DNA by pVI-MVP vaults in 264.7 RAW cells (Figure 5). For these studies, we assessed delivery of CaPi Luc DNA or the DNA encoding the green lantern fluorescent protein (CaPi GL DNA) in the presence or absence of pVI-MVP vaults. The pVI-MVP vault particles enhanced delivery of CaPi Luc DNA compared to CaPi Luc DNA alone or with vault particles lacking pVI (Figure 5A). Optimal delivery occurred using $4 \times 10^5$ to $10 \times 10^5$ pVI-MVP vaults per cell. When higher numbers of pVI-MVP vaults and/or CaPi DNA were used, lower transfection efficiencies were observed likely due to pVI toxicity. However, pVI-MVP vaults still showed higher transfection efficiencies compared to CaPi DNA alone when fewer than $2 \times 10^5$ vaults per cell were examined (data not shown). To visualize the co-delivery of CaPi GL DNA, we examined the expression of the GL protein by observing fluorescence in RAW 264.7 cells cotransfected with either Lipofectamine 2000, or pVI-MVP vaults (Figure 5B). No fluorescence was seen when control vaults (CP-MVP vaults) were used. At a higher DNA concentration (10 $\mu$g/well *vs* 2 $\mu$g/well) pVI-MVP vaults displayed higher transfection efficiencies than CaPi Luc DNA alone or Lipofectamine 2000 with Luc plasmid DNA (Figure 5C). Here the lower transfection efficiency of Lipofectamine was due to an increased cytotoxicity by Lipofectamine. pVI-MVP vaults still showed high transfection efficiencies even considering the toxicity induced by CaPi DNA. Overall we observed lower cytotoxicity of pVI-MVP vaults compared to the commercial Lipofectamine transfection agent under optimized conditions. The enhanced delivery of biomolecules by pVI-MVP vaults is likely due to the high numbers of pVI present in each pVI-MVP vault. We estimated that only 20−30 pVI were packaged inside each vault particle when the INT targeting domain was used,[43] while the direct fusion of pVI to the N-terminus of MVP provided ~78 or more pVI peptides per vault.[36]

**Disruption of Endosomes by pVI-MVP in RAW Cells.** We examined internalization of pVI-MVP and CP-MVP vaults packaged with the red fluorescent mCherry-INT fusion protein in RAW 264.7 cells (Figure 6). Vault particles without pVI (mCherry-INT/CP-MVP vaults) were colocalized with Lysotracker (green) as indicated by the presence of punctate fluorescence at 10 and 30 min following cellular uptake. This pattern was quite different when vaults containing the pVI peptide (mCherry-INT/pVI-MVP vaults) were examined. A distinct endosomal/lysosomal swelling occurred as early as 10 min after pVI-MVP vaults were added (Figure 6, left panels). Strikingly, 30 min after uptake of pVI-MVP vaults (Figure 6, right panels), the Lysotracker staining revealed few if any punctate vesicles, which is consistent with efficient disruption of endosome/lysosomes by the well-established endosomolytic activity of pVI.[42] In addition, cells incubated with pVI-MVP vaults showed morphological changes including swelling and spread of cytosol as observed

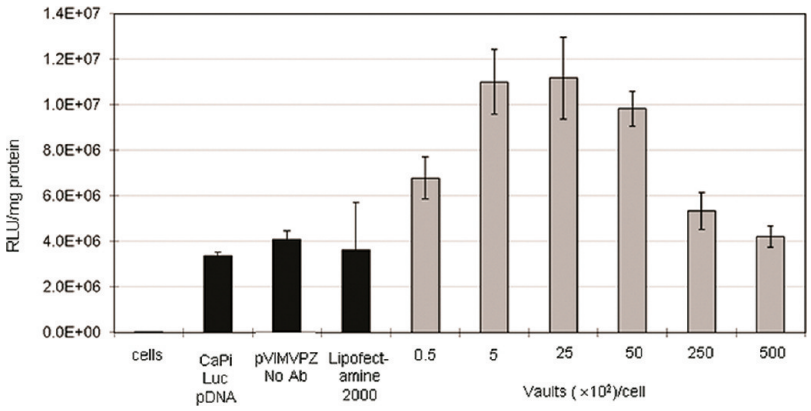


**Figure 7. Enhanced cotransfection of DNA delivery through targeted pVI-MVP-Z vault particles. A431 cells were transfected with CaPi Luc DNA (1.5 $\mu$g/well) and pVI-MVP-Z vaults prebound to anti-EGFR antibody with the indicated number of vault particles per cell (gray bars). Controls (black bars) included: CaPi Luc DNA only, CaPi Luc DNA and pVI-MVP-Z vaults without antibody ($5 \times 10^4$ particles/cell), and Luc pDNA with Lipofectamine 2000.**

during macrophage cellular response to bacterial infection.[48,49] Although quite dramatic, the cells recovered from these morphological changes and produced proteins as indicated by the transfection results (Figure 5B) which were evaluated after 72 h. These cells returned to their normal state after 72 h not only morphologically but also on the basis of their viability (data not shown).

**Multifunctional Recombinant Vaults.** With the goal of developing a bifunctional vector that can both target surface receptors and enhance cytosolic release, we designed vault particles combining these two functional motifs. To evaluate targeting and facilitated delivery without affecting cell division (as MVP-EGF vaults have been shown to stimulate receptor phosphorylation and proliferation[50,51]), we turned to vaults engineered to display the IgG binding, Z domain, on their external surface.[31,37] We fused the 20 aa lytic peptide derived from pVI to the N-terminus of MVP-Z to form pVI-MVP-Z vaults, illustrated in Figure 1C with pVI shown in red and the Z domain in blue.

As shown previously, CP-MVP-Z vaults incubated with anti-EGFR antibody showed high specific binding to A431 cells,[31] and thus we tested the transfection efficiency of these cells using pVI-MVP-Z vaults and CaPi Luc DNA (Figure 7). The pVI-MVP-Z vaults were incubated with monoclonal anti-EGFR antibody (EGFR mAb) overnight at 4 °C to allow binding of antibodies to the Z domain. Antibody bound vaults were incubated with serum starved A431 cells at 4 °C for 1 h to allow surface binding, and the cells were washed to remove unbound complexes prior to the addition of CaPi Luc DNA to the culture media and warming to 37 °C. Interestingly, the highest transfection efficiencies that we observed among all the vault particles tested in this study (pVI-MVP, pVI-INT/MVP-EGF, CP-MVP, and pVI-MVP-Z), were seen with pVI-MVP-Z antibody-targeted vaults. As seen in Figure 7, pVI-MVP-Z vault particles were quite effective at facilitating plasmid

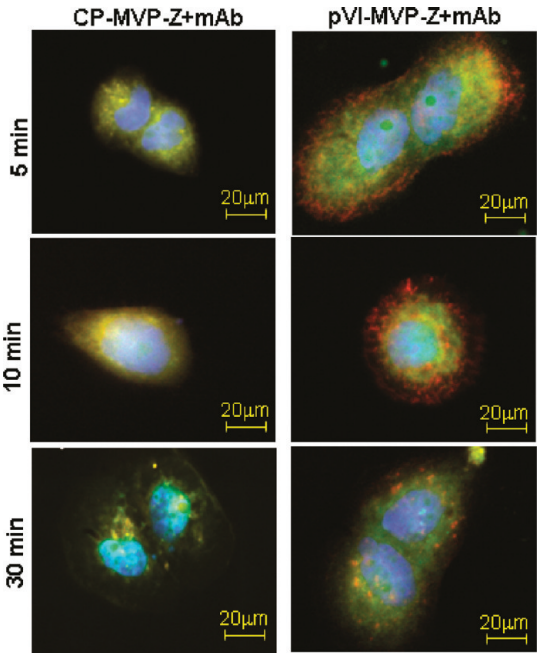


**Figure 8. Escape of pVI-MVP-Z vaults from the endosome. Comparison of A431 cells incubated with either mCherry-INT/CP-MVP-Z vaults prebound to anti-EGFR antibody or mCherry-INT/pVI-MVP-Z vaults prebound to anti-EGFR antibody for the indicated times. The nuclei were stained with Hoechst (blue). Superimposed images are shown where green fluorescence is from Lysotracker (lysosome) and red fluorescence is from the intrinsic fluorescence from the mCherry-INT protein packaged inside of the vaults. The colocalization of endosome/lysosomes and vault particles is indicated by the yellow fluorescence.**

expression per cell. As few as 50 pVI-MVP-Z+EGFR mAb vaults per cell achieved greater transfection than Lipofectamine 2000. The enhanced uptake of vaults was facilitated by the binding of the pVI-MVP-Z+EGFR mAb vaults to the EGF receptors on these cells. Higher numbers of vaults were used for the delivery of biomolecules to RAW cells (Figures 4 and 5) due to the low rate of nonspecific uptake. The uptake of vaults with

Z+EGFR mAb or EGF was enhanced owing to the high binding affinity with EGF receptors on A431 cells. An even lower concentration of vaults was required to show enhanced co-delivery of CaPi Luc DNA to A431 cells with Z+EGFR mAb or pVI-INT/MVP-EGF vaults (Figures 2 and 7). The specificity of this process was further demonstrated by preincubating A431 cells with free EGFR mAb which significantly blocked the binding of anti-EGFR-bound vaults to the cells (data not shown). This result implies that the targeted vaults are efficiently bound to EGFR, taken up by the A431 cells and, following endosomolysis, CaPi Luc DNA is co-delivered into the cytosol. CaPi Luc DNA is then transported to the nucleus where expression of the DNA occurs. Furthermore the Lipofectamine 2000 showed high toxicity in this cell line while little or no toxicity was observed with the pVI-MVP-Z+EGFR mAb vault complexes. This could be assessed by measuring the total amount of cell protein present after transfection, which with Lipofectamine 2000 was lower than that seen after pVI-MVP-Z+EGFR mAb addition (data not shown).

**Cytosolic Release of Packaged Proteins by the Interaction of pVI with Endosomal Membranes.** We monitored the endocytosis of antibody bound mCherry-INT/pVI-MVP-Z vaults in A431 cells by tracking red fluorescence (Figure 1D, Figure 8). The immediate escape of these vaults was observed in areas surrounding the outer rim of cells in less than 5 min after vault addition. This result is consistent with our previous studies which indicated that vaults containing pVI caused a rapid and progressive disruption of liposomes within ~2 min.[43] We assume that the very rapid interaction between pVI and the endosomal membranes occurred shortly after formation of the endosomal compartment. By 30 min, vaults were already released from presumed endosomes and located independently within the cytoplasm as shown by the red staining in Figure 8, while vault particles without pVI were still trapped in Lysotracker-positive compartments (presumably endosomes and early lysosomes).

It was clear from the fluorescence data (Figure 8) that significant disruptions of the endosomal membrane must have occurred in order for the fluorescent mCherry-INT protein to enter the cytoplasm. However, as was seen in the transfection experiments (Figure 7), these cells did not appear damaged by the endosome disruption induced by the pVI-MVP-Z vault. A431 cells exposed to relatively high concentrations of mCherry-INT/pVI-MVP-Z vaults were maintained in culture and observed for up to 7 days. These cells continued to display mCherry fluorescence within their cytoplasm and continued to display a normal morphology and to proliferate, indicating that the endosome disruption did not appear to be cytotoxic.

## CONCLUSIONS

These results demonstrate that vaults can be engineered to contain targeting and membrane lytic domains. These multifunctional vaults have improved therapeutic potential as they bind to cell-specific receptors with high affinity, enter *via* endocytosis, and efficiently lyse endosomal membranes with negligible toxicity. Multifunctional vaults should serve as efficient vehicles for delivery of packaged therapeutic molecules to the cytosol of specific cells.

## MATERIALS AND METHODS

**Recombinant pVI Vault Plasmids.** The pVI lytic peptide (aa 34−53, AFSWGSLWSGIKNFGSTVKN) was fused to the N-terminus of MVP. The following PCR primers were used: pVI reverse GGG GCC ATG GCG CTG CCG CGC GGC ACC AGG CCG TTC TTA ACG GTG GAA CCG and pVI forward CTC TGC TAG CCA CCA TGG CCT TCA GCT GGG GCT CG, and the template was pVI-INT.[43] All the primers used in this study were purchased from Invitrogen. The PCR product was digested with *Nco*I and ligated inframe to the same site in MVP to form pVI-MVP in pFastBac. All constructs were confirmed by DNA sequence analysis carried out by Laragen, Inc. (Los Angeles, CA). The constructs encoding EGF vaults, CP-MVP vaults, CP-MVP-Z vaults, pVI-INT, and mCherry-INT were described previously.[25,31,43] The Z domain was subcloned from CP-MVP-Z using *Xho*I and *Kpn*I and the gel purified 1 kb fragment was inserted into the same sites in pVI-MVP in pFastBac to form pVI-MVP-Z in pFastBac.

**Expression and Purification of Recombinant Vaults.** Recombinant baculoviruses were generated for pVI-MVP and pVI-MVP-Z using the Bac-to-Bac protocol (Invitrogen). For vault purification, baculovirus-infected Sf9 insect cells were subjected to a standard protocol as described previously.[24] To minimize aggregation of the pVI-MVP and pVI-MVP-Z vaults into vaultimers, the NaCl concentration in buffer A (50 mM Tris, pH 7.4, 75 mM NaCl, 0.5 mM $MgCl_2$) was reduced to 25 mM NaCl during the purification. In contrast, when pVI-INT was packaged inside of EGF vaults, the salt concentration in buffer A was increased to 150 mM NaCl. Bacterially expressed pVI-INT cell pellets were resuspended in Bugbuster (Novagen) protein extraction reagent supplemented with Benzonase (20 U/mL, Novagen), 1.0 mg/mL of lysozyme (Sigma), and one tablet of EDTA-free protease inhibitor cocktail (Roche). To package pVI-INT molecules into the interior of EGF vaults, lysates were mixed, and the mixture was incubated on ice for 30 min before performing the standard vault purification protocol.[24,33] The purified vaults were resuspended in 20 mM MES at pH 6.5 and stored at 4 °C.

**Co-delivery of CaPi DNA *via* Recombinant Vaults.** A431 and HeLa cells were grown and maintained in DMEM supplemented with 10% fetal bovine serum. Prior to transfection with pVI-INT/MVP-EGF vaults, the cells ($5\times 10^4$ cells/well) were seeded onto 24-well culture plates and incubated for 16 h without serum to deplete endogenous EGF. Variable amounts of pVI-INT/MVP-EGF vaults were added to the cells followed by a 1 h incubation at 4 °C in medium containing 0.2% serum (0.3 mL/well) to allow binding to EGFR. Unbound vaults were removed and the cells were washed three times with cold PBS, followed by the addition of the indicated amounts of CaPi DNA in medium containing 10% serum (0.4 mL/well). To allow uptake of EGF receptor bound vaults and CaPi DNA, cells were incubated at 37 °C. CaPi DNA precipitates were formed following the manufacturer's protocol (Mammalian Transfection Kit, Stratagene). Briefly 0.96 $\mu$L of 2.5 M $CaCl_2$ solution was mixed with 0.8 $\mu$g of plasmid DNA (pDNA). The mixture was incubated for 30 min at room temperature and then applied to each well for the transfection. After 24 h of incubation (4 h incubation for Lipofectamine as recommended by the manufacturer), the

medium was replaced with complete medium containing 10% serum (0.4 mL/well), followed by an additional 48 h of incubation.

For targeted transfections with pVI-MVP-Z vaults, vaults were prebound to anti-EGFR, clone LA22 monoclonal antibody (Millipore) by preincubating for 16 h at 4 °C to allow the antibodies to bind to the vaults. A431 or HeLa cells were serum starved for 1 h to remove traces of EGF in the medium. The indicated amounts of pVI-MVP-Z vaults prebound to anti-EGFR antibody were added to the cells followed by a 1 h incubation at 4 °C in medium containing 0.2% serum (0.3 mL/well) to allow binding to EGFR. Unbound vaults were removed and the cells were washed three times with cold PBS, followed by the addition of the indicated amounts of CaPi DNA in medium containing 10% serum (0.4 mL/well). To allow uptake of EGF receptor bound vaults and CaPi DNA, cells were incubated at 37 °C. CaPi DNA precipitates were formed following the manufacturer's protocol (Mammalian Transfection Kit, Stratagene). For the CaPi DNA preparation, 1.8 $\mu$L of 2.5 M $CaCl_2$ solution was mixed with 1.5 $\mu$g of pDNA. The mixture was incubated for 30 min at room temperature and then added to each well for the transfection.

For nontargeted transfection with pVI-MVP vaults, the mouse macrophage RAW 264.7 cells ($5 \times 10^4$ cell/well) were seeded on 24-well culture plates and incubated for 16 h in DMEM containing 10% FBS (0.4 mL/well) before transfection. The recombinant pVI-MVP vaults and CaPi DNA were added to the cell culture and coincubated for 24 h followed by 48 h of postincubation. Luciferase gene expression was then measured using the Luciferase Assay System (Promega) and a Lumat LB9507 luminometer (Berthold Technologies). The protein concentration in each well was determined using a Micro BCA Protein Assay Reagent Kit. The optimal conditions including the number of vault particles and CaPi DNA concentrations used for each of the protocols were determined empirically, as using too high a concentration of vault particles in some protocols were toxic to the cells.

**Vault-Mediated Endosome Penetration of Ribotoxin.** To evaluate cell membrane penetration, we measured the delivery of a ribotoxin, saporin (Sigma) into the cytosol of the murine macrophage RAW 264.7 cells *via* pVI-MVP vaults. The cells (3,000 cells/well) were seeded on a 96-well tissue culture plate and incubated overnight in DMEM containing 10% FBS. Variable amounts of vaults were applied to each well in the presence ($1.65 \times 10^{-7}$ M) or absence of saporin in DMEM for 4 h. Following incubation, the cells were washed three times with PBS buffer and cultured in medium containing 10% FBS for 48 h before measuring cell viability using a MTT assay kit (Roche). The absorbance was measured at 560 nm on a Victor$^3$ 1420 multilabel counter (PerkinElmer). All experiments were performed in triplicate. The optimal conditions including the number of vault particles and ribotoxin concentrations used for each of the protocols were determined empirically.

**Endocytosis of Recombinant Vaults.** A431 or HeLa cells ($4 \times 10^4$/well) were plated onto 12 mm glass coverslips coated with poly-L-lysine in 4-well Petri dishes and incubated at 37 °C (with 5% $CO_2$) for 16 h. Purified mCherry-INT/pVI-MVP-Z vaults (100 $\mu$g) were incubated with anti-EGFR antibody LA22 (1 $\mu$g) in PBS containing 0.05% Tween 20 (Fisher Scientific) at 4 °C for 16 h with tumbling. The cells were serum-starved for 1 h before the addition of antibody-bound vaults, followed by 1 h incubation at 4 °C in DMEM (0.25 mL containing 0.2% FBS per well) for specific membrane binding studies. Cells were washed three times with cold PBS and incubated with Lysotracker Green DND-26 (Invitrogen) at 37 °C. Then the cells were washed three times with cold PBS and fixed in 4% paraformaldehyde and nuclei stained with Hoechst 33342 (Invitrogen). Cells were mounted in Vinol 205 and visualized using fluorescent microscopy (Axio Imager Z1 microscope, Carl Zeiss). The optimal conditions including the number of vault particles used for each of the protocols were determined empirically.

*Acknowledgment.* This study was supported by grants from the National Institutes of Health awards EB-004553 (to L. Rome and V. Kickhoefer) and HL054352 (to G. Nemerow) and the National Science Foundation MCB-0210690 (to L. Rome). We thank H. Roseboro and L. Fang for excellent technical assistance.

## REFERENCES AND NOTES

1. During, M. J. Adeno-Associated Virus as a Gene Delivery System. *Adv. Drug Delivery Rev.* **1997**, *27*, 83–94.
2. Felgner, P. L.; Gadek, T. R.; Holm, M.; Roman, R.; Chan, H. W.; Wenz, M.; Northrop, J. P.; Ringold, G. M.; Danielsen, M. Lipofection: A Highly Efficient, Lipid-Mediated DNA-Transfection Procedure. *Proc. Natl. Acad. Sci. U.S.A.* **1987**, *84*, 7413–7417.
3. Felgner, P. L. Improvements in Cationic Liposomes for *in Vivo* Gene Transfer. *Hum. Gene Ther.* **1996**, *7*, 1791–1793.
4. Pedroso de Lima, M. C.; Simoes, S.; Pires, P.; Faneca, H.; Duzgunes, N. Cationic Lipid−DNA Complexes in Gene Delivery: From Biophysics to Biological Applications. *Adv. Drug Delivery Rev.* **2001**, *47*, 277–294.
5. Boussif, O.; Lezoualc'h, F.; Zanta, M. A.; Mergny, M. D.; Scherman, D.; Demeneix, B.; Behr, J. P. A Versatile Vector for Gene and Oligonucleotide Transfer into Cells in Culture and *in Vivo*: Polyethylenimine. *Proc. Natl. Acad. Sci. U.S.A.* **1995**, *92*, 7297–7301.
6. Ogris, M.; Wagner, E. Targeting Tumors with Nonviral Gene Delivery Systems. *Drug Discovery Today* **2002**, *7*, 479–485.
7. Harada-Shiba, M.; Yamauchi, K.; Harada, A.; Takamisawa, I.; Shimokado, K.; Kataoka, K. Polyion Complex Micelles as Vectors in Gene Therapy—Pharmacokinetics and *in Vivo* Gene Transfer. *Gene Ther.* **2002**, *9*, 407–414.
8. Cappello, J.; Crissman, J.; Dorman, M.; Mikolajczak, M.; Textor, G.; Marquet, M.; Ferrari, F. Genetic Engineering of Structural Protein Polymers. *Biotechnol. Prog.* **1990**, *6*, 198–202.
9. Mahat, R. I.; Monera, O. D.; Smith, L. C.; Rolland, A. Peptide-Based Gene Delivery. *Curr. Opin. Mol. Ther.* **1999**, *1*, 226–243.
10. Chowdhury, E. H.; Akaike, T. Bio-Functional Inorganic Materials: an Attractive Branch of Gene-Based Nano-Medicine Delivery for 21st Century. *Curr. Gene Ther.* **2005**, *5*, 669–676.
11. Kakizawa, Y.; Miyata, K.; Furukawa, S.; Kataoka, K. Size-Controlled Formation of a Calcium Phosphate-Based Organic−Inorganic Hybrid Vector for Gene Delivery Using Poly(ethylene glycol)-block-Poly(aspartic acid). *Adv. Mater.* **2004**, *16*, 699–702.
12. Lundstrom, K. Latest Development in Viral Vectors for Gene Therapy. *Trends Biotechnol.* **2003**, *21*, 117–122.
13. Fischer, D.; Bieber, T.; Li, Y.; Elsasser, H. P.; Kissel, T. A Novel Nonviral Vector for DNA Delivery Based on Low Molecular Weight, Branched Polyethylenimine: Effect of Molecular Weight on Transfection Efficiency and Cytotoxicity. *Pharm. Res.* **1999**, *16*, 1273–1279.
14. Plank, C.; Mechtler, K.; Szoka, F. C., Jr.; Wagner, E. Activation of the Complement System by Synthetic DNA Complexes: A Potential Barrier for Intravenous Gene Delivery. *Hum. Gene Ther.* **1996**, *7*, 1437–1446.
15. Merdan, T.; Kunath, K.; Fischer, D.; Kopecek, J.; Kissel, T. Intracellular Processing of Poly(ethylene imine)/Ribozyme Complexes Can Be Observed in Living Cells by Using Confocal Laser Scanning Microscopy and Inhibitor Experiments. *Pharm. Res.* **2002**, *19*, 140–146.
16. Mesnil, M.; Yamasaki, H. Bystander Effect in Herpes Simplex Virus−Thymidine Kinase/Ganciclovir Cancer Gene Therapy: Role of Gap-Junctional Intercellular Communication. *Cancer Res.* **2000**, *60*, 3989–3999.
17. Suprenant, K. A. Vault Ribonucleoprotein Particles: Sarcophagi, Gondolas, or Safety Deposit Boxes? *Biochemistry* **2002**, *41*, 14447–14454.
18. Kedersha, N. L.; Heuser, J. E.; Chugani, D. C.; Rome, L. H. Vaults. III. Vault Ribonucleoprotein Particles Open into Flower-like Structures with Octagonal Symmetry. *J. Cell Biol.* **1991**, *112*, 225–235.
19. Kickhoefer, V. A.; Siva, A. C.; Kedersha, N. L.; Inman, E. M.; Ruland, C.; Streuli, M.; Rome, L. H. The 193-kD Vault Protein, VPARP, Is a Novel Poly(ADP-ribose) Polymerase. *J. Cell Biol.* **1999**, *146*, 917–928.
20. Kickhoefer, V. A.; Stephen, A. G.; Harrington, L.; Robinson, M. O.; Rome, L. H. Vaults and Telomerase Share a Common Subunit, TEP1. *J. Biol. Chem.* **1999**, *274*, 32712–32717.
21. Kickhoefer, V. A.; Searles, R. P.; Kedersha, N. L.; Garber, M. E.; Johnson, D. L.; Rome, L. H. Vault Ribonucleoprotein Particles from Rat and Bullfrog Contain a Related Small RNA

That Is Transcribed by RNA Polymerase III. *J. Biol. Chem.* **1993**, *268*, 7868–7873.
22. Kickhoefer, V. A.; Rajavel, K. S.; Scheffer, G. L.; Dalton, W. S.; Scheper, R. J.; Rome, L. H. Vaults Are Up-Regulated in Multidrug-Resistant Cancer Cell Lines. *J. Biol. Chem.* **1998**, *273*, 8971–8974.
23. van Zon, A.; Mossink, M. H.; Schoester, M.; Scheffer, G. L.; Scheper, R. J.; Sonneveld, P.; Wiemer, E. A. Multiple Human Vault RNAs. Expression and Association with the Vault Complex. *J. Biol. Chem.* **2001**, *276*, 37715–37721.
24. Stephen, A. G.; Raval-Fernandes, S.; Huynh, T.; Torres, M.; Kickhoefer, V. A.; Rome, L. H. Assembly of Vault-like Particles in Insect Cells Expressing Only the Major Vault Protein. *J. Biol. Chem.* **2001**, *276*, 23217–23220.
25. Mikyas, Y.; Makabi, M.; Raval-Fernandes, S.; Harrington, L.; Kickhoefer, V. A.; Rome, L. H.; Stewart, P. L. Cryoelectron Microscopy Imaging of Recombinant and Tissue Derived Vaults: Localization of the MVP N Termini and VPARP. *J. Mol. Biol.* **2004**, *344*, 91–105.
26. Anderson, D. H.; Kickhoefer, V. A.; Sievers, S. A.; Rome, L. H.; Eisenberg, D. Draft Crystal Structure of the Vault Shell at 9-A Resolution. *PLoS Biol.* **2007**, *5*, e318.
27. Kickhoefer, V. A.; Garcia, Y.; Mikyas, Y.; Johansson, E.; Zhou, J. C.; Raval-Fernandes, S.; Minoofar, P.; Zink, J. I.; Dunn, B.; Stewart, P. L.; *et al.* Engineering of Vault Nanocapsules with Enzymatic and Fluorescent Properties. *Proc. Natl. Acad. Sci. U.S.A.* **2005**, *102*, 4348–4352.
28. Ng, B. C.; Yu, M.; Gopal, A.; Rome, L. H.; Monbouquette, H. G.; Tolbert, S. H. Encapsulation of Semiconducting Polymers in Vault Protein Cages. *Nano Lett.* **2008**, *8*, 3503–3509.
29. Yu, M.; Ng, B. C.; Rome, L. H.; Tolbert, S. H.; Monbouquette, H. G. Reversible pH Lability of Cross-Linked Vault Nanocapsules. *Nano Lett.* **2008**, *8*, 3510–3515.
30. Champion, C. I.; Kickhoefer, V. A.; Liu, G.; Moniz, R. J.; Freed, A. S.; Bergmann, L. L.; Vaccari, D.; Raval-Fernandes, S.; Chan, A. M.; Rome, L. H.; *et al.* A Vault Nanoparticle Vaccine Induces Protective Mucosal Immunity. *PLoS One* **2009**, *4*, e5409.
31. Kickhoefer, V. A.; Han, M.; Raval-Fernandes, S.; Poderycki, M. J.; Moniz, R. J.; Vaccari, D.; Silvestry, M.; Stewart, P. L.; Kelly, K. A.; Rome, L. H. Targeting Vault Nanoparticles to Specific Cell Surface Receptors. *ACS Nano* **2009**, *3*, 27–36.
32. Goldsmith, L. E.; Yu, M.; Rome, L. H.; Monbouquette, H. G. Vault Nanocapsule Dissociation into Halves Triggered at Low pH. *Biochemistry* **2007**, *46*, 2865–2875.
33. Poderycki, M. J.; Kickhoefer, V. A.; Kaddis, C. S.; Raval-Fernandes, S.; Johansson, E.; Zink, J. I.; Loo, J. A.; Rome, L. H. The Vault Exterior Shell Is a Dynamic Structure That Allows Incorporation of Vault-Associated Proteins into Its Interior. *Biochemistry* **2006**, *45*, 12184–12193.
34. Esfandiary, R.; Kickhoefer, V. A.; Rome, L. H.; Joshi, S. B.; Middaugh, C. R. Structural Stability of Vault Particles. *J. Pharm. Sci.* **2009**, *98*, 1376–1386.
35. Yang, J.; Kickhoefer, V. A.; Ng, B. C.; Gopal, A.; Bentolila, L. A.; John, S.; Tolbert, S. H.; Rome, L. H. Vaults Are Dynamically Unconstrained Cytoplasmic Nanoparticles Capable of Half Vault Exchange. *ACS Nano* **2010**, *4*, 7229–7240.
36. Tanaka, H.; Kato, K.; Yamashita, E.; Sumizawa, T.; Zhou, Y.; Yao, M.; Iwasaki, K.; Yoshimura, M.; Tsukihara, T. The Structure of Rat Liver Vault at 3.5 Angstrom Resolution. *Science* **2009**, *323*, 384–388.
37. Nilsson, B.; Moks, T.; Jansson, B.; Abrahmsen, L.; Elmblad, A.; Holmgren, E.; Henrichson, C.; Jones, T. A.; Uhlen, M. A Synthetic IgG-Binding Domain Based on Staphylococcal Protein A. *Protein Eng.* **1987**, *1*, 107–113.
38. van Zon, A.; Mossink, M. H.; Schoester, M.; Scheffer, G. L.; Scheper, R. J.; Sonneveld, P.; Wiemer, E. A. Structural Domains of Vault Proteins: A Role for the Coiled Coil Domain in Vault Assembly. *Biochem. Biophys. Res. Commun.* **2002**, *291*, 535–541.
39. Kozlov, G.; Vavelyuk, O.; Minailiuc, O.; Banville, D.; Gehring, K.; Ekiel, I. Solution Structure of a Two-Repeat Fragment of Major Vault Protein. *J. Mol. Biol.* **2006**, *356*, 444–452.
40. Kar, U. K.; Srivastava, M. K.; Andersson, A.; Baratell, F.; Huang, M.; Kickhoefer, V. A.; Dubinett, S. M.; Rome, L. H.; Sharma, S. Novel CCL21-Vault Nanocapsule Intratumoral Delivery Inhibits Lung Cancer Growth. *PLoS One* **2011**, in press, DOI: 10.1371/journal.pone.0018758.
41. Buehler, D. C.; Toso, D. B.; Kickhoefer, V. A.; Hong Zhou, Z.; Rome, L. H. Vaults Engineered for Hydrophobic Drug Delivery. *Small* **2011**, in press, DOI: 10.1002/smll.201002274.
42. Wiethoff, C. M.; Wodrich, H.; Gerace, L.; Nemerow, G. R. Adenovirus Protein VI Mediates Membrane Disruption Following Capsid Disassembly. *J. Virol.* **2005**, *79*, 1992–2000.
43. Lai, C. Y.; Wiethoff, C. M.; Kickhoefer, V. A.; Rome, L. H.; Nemerow, G. R. Vault Nanoparticles Containing an Adenovirus-Derived Membrane Lytic Protein Facilitate Toxin and Gene Transfer. *ACS Nano* **2009**, *3*, 691–699.
44. Seiler, M. P.; Gottschalk, S.; Cerullo, V.; Ratnayake, M.; Mane, V. P.; Clarke, C.; Palmer, D. J.; Ng, P.; Rooney, C. M.; Lee, B. Dendritic Cell Function after Gene Transfer with Adenovirus–Calcium Phosphate Co-Precipitates. *Mol. Ther.* **2007**, *15*, 386–392.
45. Eisenstein, M. A. Look Back: Fast, Cheap and Under Control. *Nat. Methods* **2005**, *2*, 318–318.
46. Varga, C. M.; Tedford, N. C.; Thomas, M.; Klibanov, A. M.; Griffith, L. G.; Lauffenburger, D. A. Quantitative Comparison of Polyethylenimine Formulations and Adenoviral Vectors in Terms of Intracellular Gene Delivery Processes. *Gene Ther.* **2005**, *12*, 1023–1032.
47. Moyer, C. L.; Wiethoff, C. M.; Maier, O.; Smith, J. G.; Nemerow, G. R. Functional Genetic and Biophysical Analyses of Membrane Disruption By Human Adenovirus. *J. Virol.* **2011**, *85*, 2631–2641.
48. Shaughnessy, L. M.; Hoppe, A. D.; Christensen, K. A.; Swanson, J. A.Membrane Perforations Inhibit Lysosome Fusion by Altering pH and Calcium in Listeria Monocytogenes Vacuoles. *Cell Microbiol.* **2006**, *8*, 781–792.
49. Kingdon, G. C.; Sword, C. P. Effects of Listeria Monocytogenes Hemolysin on Phagocytic Cells and Lysosomes. *Infect. Immun.* **1970**, *1*, 356–362.
50. Xie, H.; Pallero, M. A.; Gupta, K.; Chang, P.; Ware, M. F.; Witke, W.; Kwiatkowski, D. J.; Lauffenburger, D. A.; Murphy-Ullrich, J. E.; Wells, A. EGF Receptor Regulation of Cell Motility: EGF Induces Disassembly of Focal Adhesions Independently of the Motility-Associated PLCgamma Signaling Pathway. *J. Cell Sci.* **1998**, *111*, 615–624.
51. Wells, A. EGF Receptor. *Int. J. Biochem. Cell Biol.* **1999**, *31*, 637–643.